Progress In Electromagnetics Research M, Vol. 101, 89–100, 2021

Research on the Model and Characteristics of Underground Magnetic Induction Communication Channel

Bao Heng Liu*, **Tian Hui Fu, and Yong Bin Wang**

Abstract—The traditional electromagnetic wave wireless communication in the underground environment has the problem of unstable channel path loss, large antenna size, high path loss, etc. To address these issues, the channel models of magnetic induction communication and magnetic induction waveguide communication based on quasi-static field coupling are proposed, and the characteristics of magnetic field strength, path loss, bandwidth, and channel capacity are analyzed in detail. The results show that the magnetic induction communication system channel is stable, compared with the ordinary induction communication, and the path loss of magnetic induction waveguide communication is reduced a lot, even in the case of high noise and transmission distance increased by more than 20 times. But the bandwidths of the two ways are small and similar. The path loss and bandwidth decide the system capacity, and system capacity is also affected by the number of turns, working frequency, coil resistance, and size.

1. INTRODUCTION

Magnetic induction communication realizes the transmission of information by coupling the quasi-static magnetic field [1]. Because the permeability is almost the same in complex geological media, the transmitting antenna and receiving antenna adopt the small size coil with much smaller radiation resistance than the electric dipole, thus the magnetic induction communication technology solve the problem of unstable transmission channel, large antenna size, and multipath effect in traditional electromagnetic communication [2–6]. The magnetic induction waveguide technique introduces a certain number of passive relay coils between the transceiver coils and receiving coils. Signals and energy are transmitted through magnetic coupling of some resonant coils. It can solve the problem of high path loss in common magnetic induction communication, and relay coil has the advantages of no energy consumption, low cost, easy deployment and maintenance [7–9]. Thus, it can be seen that magnetic induction communication is an underground wireless communication method with significant advantages and great prospects. To meet the application demand of wireless underground communication network, this paper constructs magnetic induction communication and magnetic induction waveguide models, and deeply analyzes and studies the channel characteristics such as magnetic field strength, path loss, link budget, bandwidth capacity, and bit error rate.

2. CHANNEL MODEL

2.1. Magnetic Induction Communication Channel Model

In the magnetic induction communication system, transmission and reception are completed through multi-turn coils. As shown in Fig. 1(a), a_t and a_r are the radii of the transmitting coil and receiving coil,

Received 8 January 2021, Accepted 7 February 2021, Scheduled 23 February 2021
* Corresponding author: Bao Heng Liu (1094480943@qq.com).
The authors are with the College of Electronic Engineering, Naval University of Engineering, Wuhan, Hubei 430033, China.

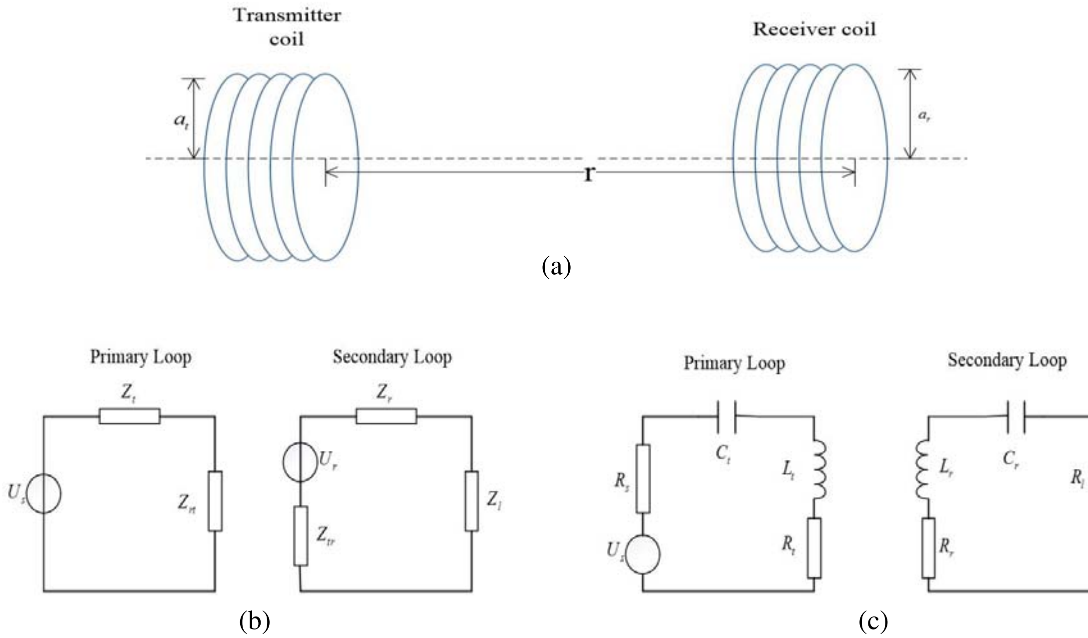

Figure 1. (a) MI system and equivalent circuit models (b) and (c).

respectively, and r is the distance between them. If the sinusoidal current is fed into the transmitting coil, that is, $I = I_0 \cdot e^{-jwt}$, the receiving coil generates sinusoidal current due to the interaction between two coupling coils, thus realizing information transmission. As shown in Figs. 1(b) and (c), two equivalent circuit models are established [8–13].

In model 1 in Fig. 1(b) [8]:

$$Z_t = R_t + j\omega L_t \quad Z_{rt} = \frac{\omega^2 M^2}{R_r + j\omega L_r + Z_l} \quad Z_r = R_r + j\omega L_r$$
$$Z_{tr} = \frac{\omega^2 M^2}{R_t + j\omega L_t} \quad U_r = -j\omega M \frac{U_s}{R_t + j\omega L_t} \tag{1}$$

where R_t and R_r are resistances of transmitting and receiving coils, respectively; L_t and L_r are self-inductances of the two; Z_t and Z_r are self-impedances of the two; Z_{rt} is the influence of receiving coil on transmitting coil; Z_{tr} is the influence of transmitting coil on receiving coil; M is mutual inductance between the two; Z_l is the load impedance; U_s is the transmitter voltage; U_r is the inductive voltage of receiving coil.

The transmitting power P_t is the power consumed by the main circuit, and the receiving power P_r is the power consumed by the load impedance Z_l. To maximize the receiving power, the load impedance is designed as the complex conjugate of the output impedance of the secondary circuit. When a low resistance loop with high frequency and multiple turns is adopted, the receiving power P_r is [8]:

$$P_r \simeq \frac{P_t \omega \mu N_r a_t^3 a_r^3}{16 R_0 r^6} \tag{2}$$

where R_0 is the resistance per unit length of the wire, μ the permeability of the earth, and N_r the number of turns of the transmitting loop.

In model 2 in Fig. 1(c), C_t and C_r are capacitances of transmitting and receiving coils, respectively; R_l is the load impedance; R_s is the power resistance. The receiving power P_r is [11–13]:

$$P_r = P_t Q_t Q_r \eta_t \eta_r \frac{a_t^3 a_r^3 \pi^2}{N_t N_r \left(a_t^2 + r^2\right)^3} \tag{3}$$

where $Q_t = \omega L_t / R_t$ and $Q_r = \omega L_r / R_r$ are the quality factors of transmitting and receiving coils, respectively; $\eta_t = R_s/(R_s + R_t)$ and $\eta_r = R_l/(R_l + R_r)$ are the efficiencies of transmitting and receiving coils, respectively. If $R_s \gg R_t$ and $R_l \gg R_r$, the transmitting coil radius a_t is far less than the communication distance r, then the received power P_r can be expressed as [10]:

$$P_r \simeq \frac{P_t \omega^2 \mu^2 a_t^3 a_r^3}{16 N_r N_t R_0^2 r^6} \tag{4}$$

2.2. Magnetic Induction Waveguide Communication Channel Model

As shown in Fig. 2, the magnetic induction waveguide is modeled as a multi-stage transformer, and the distance r between the two coils is much greater than the radius a of the coils, so just considering the mutual inductance between adjacent coils [9]. By adding capacitance to each coil, the resonant coil can be formed by designing the appropriate capacitance value, which can effectively transmit the signal.

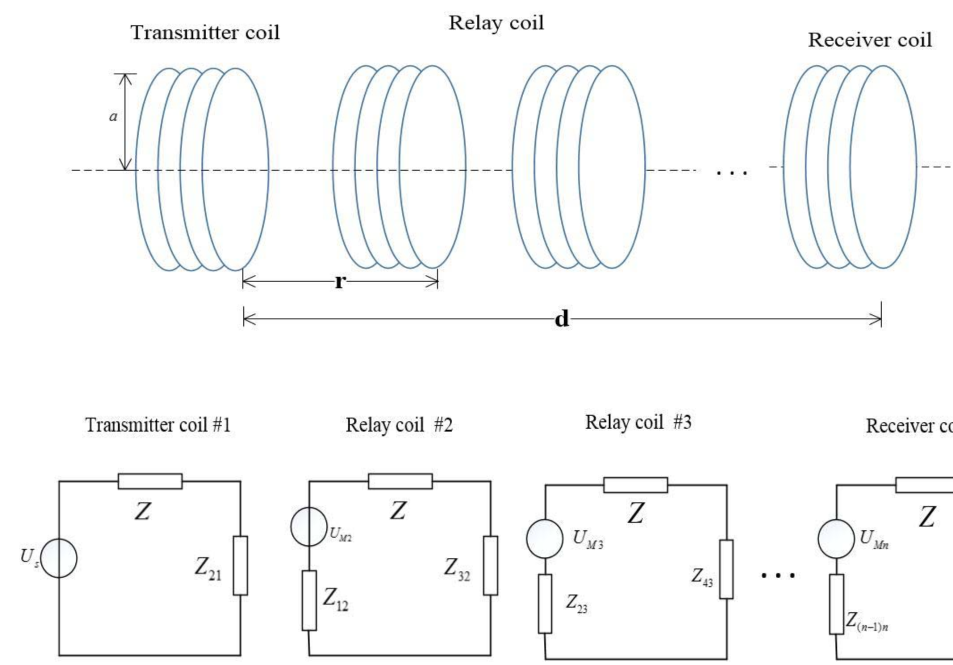

Figure 2. MI waveguide system model.

If the sending and receiving coils and relay coil all use the same design parameters such as number of turns, impedance, matching capacitance, and self-induction, then the power P_r of the receiving coil is [8, 9]:

$$P_r = \frac{1}{4(Z_{(n-1)n} + R)} \cdot \frac{U_s^2}{\zeta^2\left(\frac{R}{\omega M}, n-1\right)}, \quad Z_{(i-1)i} = \frac{\omega^2 M^2}{Z + Z_{(i-2)(i-1)}} \left(i = 3, 4, \ldots, n \ Z_{12} = \frac{\omega^2 M^2}{Z}\right)$$

$$Z = R + j\omega L + \frac{1}{j\omega C} \tag{5}$$

$$\zeta^2\left(\frac{R}{\omega M}, n-1\right) = b_{n-1}\left(\frac{R}{\omega M}\right)^{n-1} + b_{n-2}\left(\frac{R}{\omega M}\right)^{n-2} + \ldots + b_2\left(\frac{R}{\omega M}\right)^2 + b_1\left(\frac{R}{\omega M}\right) + b_0 \tag{6}$$

where $Z_{(i-1)i}$ is the reflection impedance generated by the $(i-1)$ coil on the i coil, L the self-inductance of coils, R the impedance of coils, C the matching capacitance, N the winding turns, n the total number of coils, and $\{b_i, i = 0, 1, 2, 3, \ldots, n-1\}$ are the polynomial coefficients.

3. CHANNEL CHARACTERISTIC RESEARCH AND SIMULATION ANALYSIS.

This paper uses MATLAB to simulate and analyze the channel characteristics of magnetic induction and magnetic induction waveguide communication system. Assuming that all the coil parameters are the same, set radius of 0.1 m, coil number of turns N of 10, per unit length of wire coil impedance R_0 of 0.02 Ω/m, frequency f of 10 MHZ, and current I of 1 A.

3.1. Magnetic Field Intensity

Figures 3(a) and (b) respectively show the circular coil buried at depth h and the circular coil located at ground height h_0. Establish a cylindrical coordinate system (ρ, φ, z).

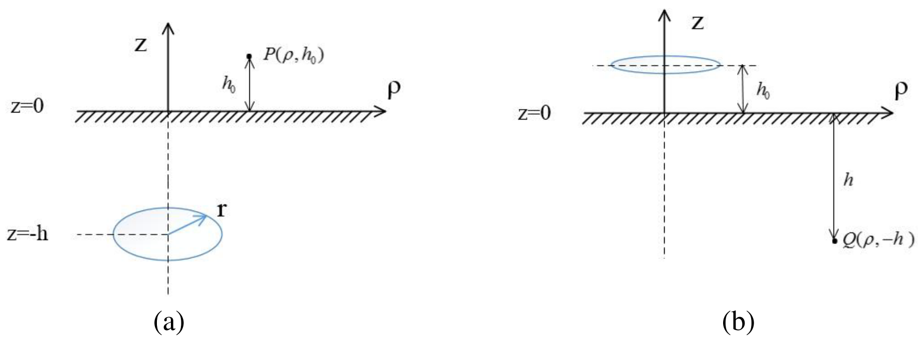

Figure 3. (a) Loop antenna buried in earth at depth h. (b) Loop antenna located above ground with height h_0.

The observation point P is located at the altitude h_0 and the radial coordinate ρ, and the magnetic field generated by the buried circular coil is [14]:

$$H_{z0} = -\frac{INS}{2\pi h^3}Q_0 \quad H_{\rho 0} = \frac{INS}{2\pi h^3}P_0 \tag{7}$$

where S is the coil area, and P_0 and Q_0 are transmission losses caused by attenuation of the conductive ground [15].

$$Q_0 = \int_0^\infty \frac{x^3 e^{-(x^2+jH^2)^{1/2}+x(1-Z)} J_0(xD)dx}{x+(x^2+jH^2)^{1/2}} \tag{8}$$

$$P_0 = \int_0^\infty \frac{x^3 e^{-(x^2+jH^2)^{1/2}+x(1-Z)} J_1(xD)dx}{x+(x^2+jH^2)^{1/2}} \tag{9}$$

where $D = \rho/h$, $Z = z/h$, and $H = (\mu\omega\sigma)^{1/2}h$. H is the ratio of source depth to skin depth. J_0 and J_1 are Bessel functions of the first kind.

The observation point Q is located at depth h ($z = -h$), the radial coordinate ρ, where the magnetic field generated by the circular coil on the ground is [14]:

$$H_\rho = -\frac{INS}{2\pi h^3}P \quad H_z = \frac{INS}{2\pi h^3}Q \tag{10}$$

where

$$P = \int_0^\infty \frac{J_1(Ax)}{\frac{Ax}{2}} \frac{x^2(x^2+jH^2)^{1/2} e^{-(x^2+jH^2)^{1/2}-Zx} J_1(xD)dx}{x+(x^2+jH^2)^{1/2}} \tag{11}$$

$$Q = \int_0^\infty \frac{J_1(Ax)}{\frac{Ax}{2}} \frac{x^3 e^{-(x^2+jH^2)^{1/2}-Zx} J_0(xD)dx}{x+(x^2+jH^2)^{1/2}} \tag{12}$$

where $A = a/h$, and $Z = h_0/h$.

To observe the difference between the vertical component of the magnetic field generated by the uplink loop and the downlink loop, both loops measure the vertical component of the magnetic field at the same distance (10 m) from the transmitting loop. Fig. 4 is obtained from Equations (7) and (10), and Fig. 4 shows the magnitude of the vertical component of the magnetic field generated by the underground loop relative to the surface loop when the frequency is 1–10 MHz under the condition of low and high earth conductivities.

As can be seen from Fig. 4, under the same transmission distance, the vertical component of the magnetic field generated by the underground loop is larger. For the earth with low conductivity, the difference between the two is small, but for the earth with high conductivity, the difference is large.

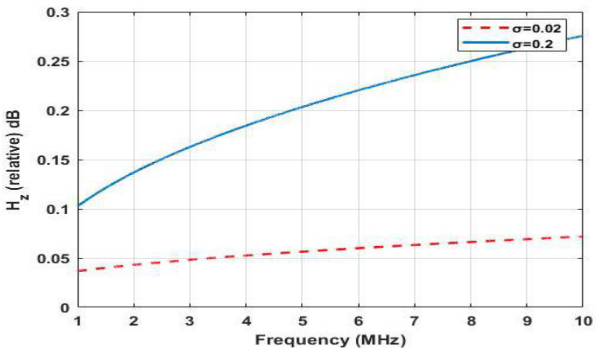

Figure 4. Comparison of surface and underground transmitted fields at 10 m separation for different earth conductivity values.

3.2. Path Loss and Link Budget

The transmitting power of the magnetic induction communication system consists of the induction power consumed by the receiving coil and the power consumed by the coil resistance, since the magnetic induction communication is realized through the near-field coupling. The coil resistance is small, and the radiated power is small, so the limited transmitted energy will not be wasted on the radiation in the surrounding space, and most of the power is transferred to the receiving coil.

According to Equations (2) and (4), the path losses of magnetic induction model 1 and model 2 respectively are:

$$L_{MI1}(r) = -10\lg\frac{P_r}{P_t} \simeq -10\lg\frac{\omega\mu N_r a_t^3 a_r^3}{16R_0 r^6} \tag{13}$$

$$L_{MI2}(r) = -10\lg\frac{P_r}{P_t} \simeq -10\lg\frac{\omega^2\mu^2 a_t^3 a_r^3}{16N_r N_t R_0^2 r^6} \tag{14}$$

The path loss of electromagnetic wave in soil is [16]:

$$L_{EM}(r) = -10\lg\frac{P_r}{P_t} \simeq 6.4 + 20\lg r + 20\lg\beta + 8.69\alpha r \tag{15}$$

where $\alpha = \omega\sqrt{\mu\varepsilon}[\frac{1}{2}(\sqrt{1+(\frac{\sigma}{\omega\varepsilon})^2}-1)]^{\frac{1}{2}}$, $\beta = \omega\sqrt{\mu\varepsilon}[\frac{1}{2}(\sqrt{1+(\frac{\sigma}{\omega\varepsilon})^2}+1)]^{\frac{1}{2}}$ [16].

The result of MATLAB calculation from Equations (13)–(15) is shown in Fig. 5. Fig. 5 shows that the two magnetic induction models have similar path losses, and the path loss of magnetic induction communication is approximately a lg function of distance r, while the path loss of electromagnetic wave system mainly comes from material absorption loss, so it is an approximately linear function of distance r. The conductivity has a great influence on the propagation of the electromagnetic wave. When the conductivity is large, the path loss of the electromagnetic wave is obviously greater than that of magnetic induction communication. Even in low conductivity environments, when the transmission distance is long enough, the magnetic induction system can have less path loss than the electromagnetic wave.

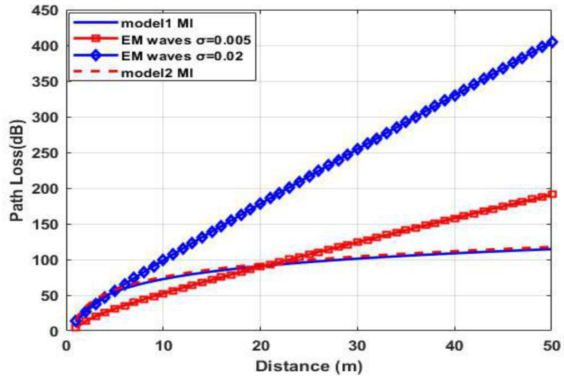

Figure 5. Path loss of the EM wave system and two models of the magnetic induction communication system.

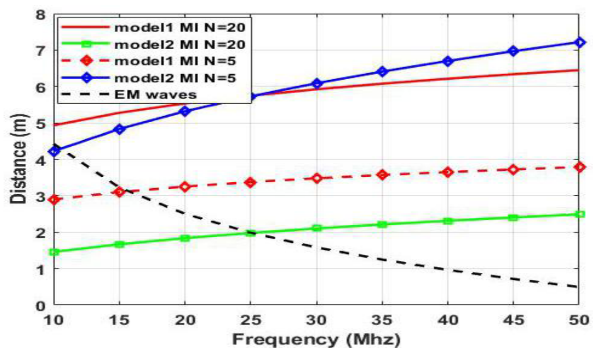

Figure 6. Link budget of the EM wave system and two models of the magnetic induction communication system.

According to Equations (13)–(15), the link budget of magnetic induction model 1, model 2 and the electromagnetic wave can be obtained, as shown in Fig. 6.

As can be seen from Fig. 6, with the increase of working frequency, the transmission distance of the magnetic induction system increases, while the transmission distance of electromagnetic wave decreases, and electromagnetic wave works more efficiently at lower frequencies, while magnetic induction works better at higher frequencies. As the number of turns increases, the transmission distance of magnetic induction model 1 increases, while the transmission distance of model 2 decreases. Therefore, model 1 is suitable for the case of multiple turns, while model 2 is more suitable for the case of low turns.

We can know from Equation (5) that for the magnetic induction waveguide system, path loss can usually be reduced by reducing the ratio of the coil distance to the coil radius, increasing the operating frequency or the number of turns of the coil, and reducing the wire resistance. However, reducing the ratio between the coil distance and coil radius will increase the difficulty of equipment deployment, and due to the constraints of matching capacitance, the working frequency and the number of turns of the coil cannot be increased without limit. Reducing the wire resistance will increase the cost, and too low resistance will cause the signal fluctuation in the band; therefore, these parameters should be balanced to achieve the best performance of the system.

According to Equation (5), the path loss of the magnetic induction waveguide system can be obtained, as shown in Fig. 7.

Figure 7(a) shows that compared with the common magnetic induction system, magnetic induction waveguide path loss can be greatly reduced and can be further reduced by reducing the distance and resistance of the relay coil. Fig. 7(b) shows the path losses of the magnetically induced waveguide system with a different number of repeating coils. It can be found that when the transmission distance is relatively close (< 40 m), increasing the number of repeating coils will have no obvious effect and cause greater path loss. When the transmission distance is large, increasing the number of repeating coils will have a good effect on reducing the path loss.

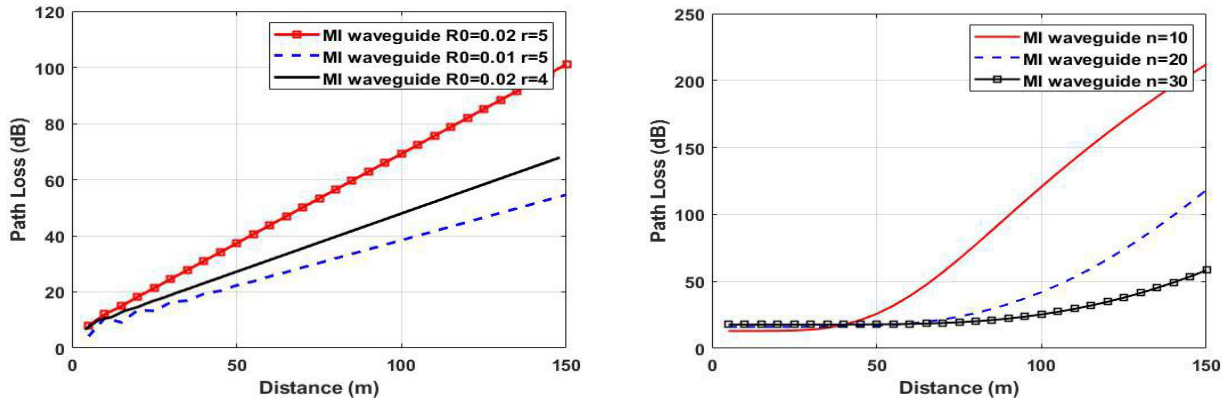

(a) (b)

Figure 7. (a) Path loss of the MI waveguide system with different wire resistance and relay distance. (b) Path loss of the MI waveguide system with different coil number.

3.3. Bit Error Rate

Bit error rate mainly depends on the three factors of path loss, noise, and system modulation mode. Assuming that the noise power is 83 dBm in the case of high noise, 103 dBm in the case of low noise, the transmitting power P_t is set as 10 dBm, and 2PSK is adopted in the modulation mode.

Figures 8(a) and (b) respectively show the bit error rate of magnetic induction system model 1, model 2, and electromagnetic wave system under low noise and high noise conditions. The bit error rate of model 1 is similar to that of model 2, and the bit error rate of model 1 is smaller. In the case of low noise, the transmission distance of the magnetic induction system is greater than that of the electromagnetic wave system regardless of the conductivity. In the case of high noise, the transmission distance of the magnetic induction system is between the electromagnetic wave systems with low conductivity and high conductivity.

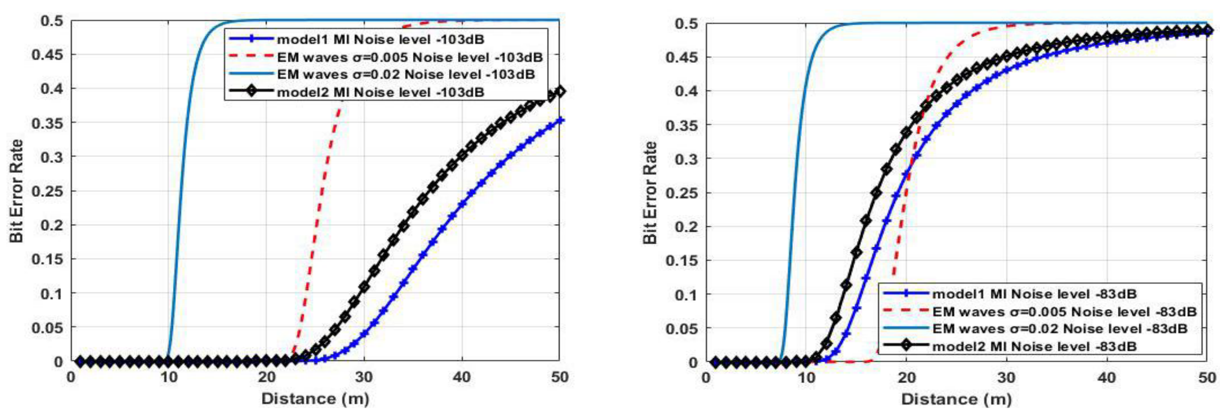

(a) (b)

Figure 8. (a) Bit error rate under low noise. (b) Bit error rate under high noise.

Figure 9 shows the relationship between bit error rate and transmission distance of the magnetic induction waveguide system with different coil numbers, resistance, and spacing under high noise. It can be seen from the figure that even in the case of high noise, the transmission range of the magnetic induction waveguide system is more than 20 times higher than that of the magnetic induction system and electromagnetic wave system. By analyzing the bit error rate, the transmission distance can be improved by reducing the distance and resistance of the loop or increasing the number of the loops.

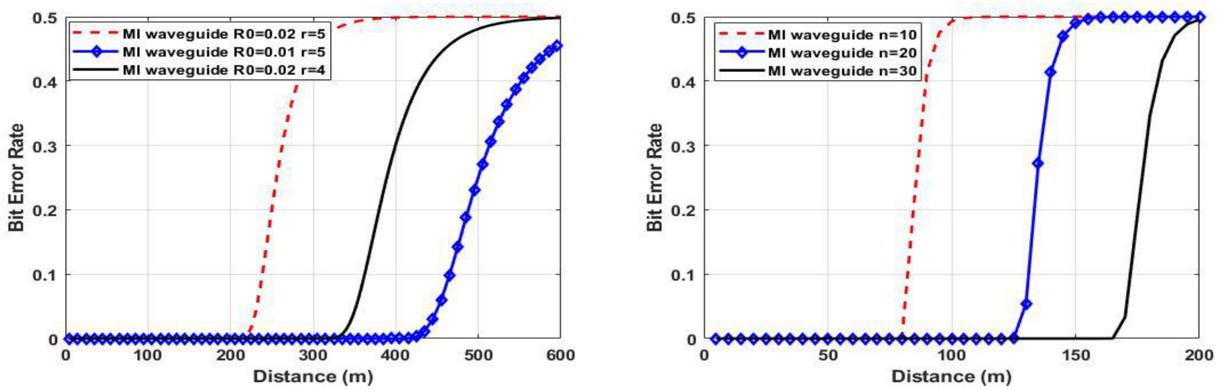

(a) (b)

Figure 9. (a) The bit error rate of the MI waveguide system with different wire resistance and relay distance. (b) The bit error rate of the MI waveguide system with different coil number.

3.4. Bandwidth and System Capacity

In a magnetic induction communication system, only a center frequency can realize secondary loop output impedance of the load matching, and any deviation from the central frequency will cause power reflection and increase path loss. Similarly, in a magnetically induced waveguide system, only one central frequency can make all coils reach the resonant state. Any deviation from the central frequency will make the resonant state disappear, and the load does not match the system. Therefore, it is necessary to analyze the bandwidth of the magnetic induction system and magnetic induction waveguide system.

Figure 10(a) shows the frequency response of the magnetic induction communication at the transmission distance of 5 m. It can be seen from the figure that the 3 dB bandwidth of the system is about 2 kHz, which is much smaller than the electromagnetic wave system. Fig. 10(b) shows the frequency response of the magnetic induction waveguide system at the transmission distance of 100 m at different relay distances and different line resistances. The results show that the 3 dB bandwidth of the magnetic induction waveguide system is similar to that of the common magnetic induction system. The lower line resistance can reduce the path loss, but it will increase the frequency response fluctuation in the band. The reduction of the relay distance can increase the bandwidth, but it also means that more repeating coils need to be deployed, which increases the cost and difficulty of deployment.

According to Shannon's theorem, channel capacity can be expressed as:

$$C = B\log_2\left(\frac{P_r}{N_0}+1\right) \tag{16}$$

where B is the channel bandwidth; 3 dB bandwidth is selected as the channel bandwidth in this paper; P_r is the received power; and N_0 is the total noise and interference power.

The capacity of the magnetic induction system is [12]:

$$C = \frac{0.644}{Q} f_0 \log_2\left(\frac{P_r}{N_0}+1\right) \tag{17}$$

where Q is the quality factor of the coil, and f_0 is the center operating frequency. If the transmitting power is set at 10 dBm, the noise power set at -105 dBm, and the received power given by Equations (2) and (4), then the channel capacities of model 1 and model 2 of the magnetic induction system are shown in Fig. 11.

Figure 11(a) shows that with the increase of transmission distance, channel capacity is reduced, that the capacities of the two models are similar, and that model 1 is larger. Fig. 11(b) shows the influence of wire resistance and frequency on channel capacity. The results show that frequency has less influence on channel capacity, while wire resistance has more influence on capacity. Channel capacity can be improved by increasing wire resistance.

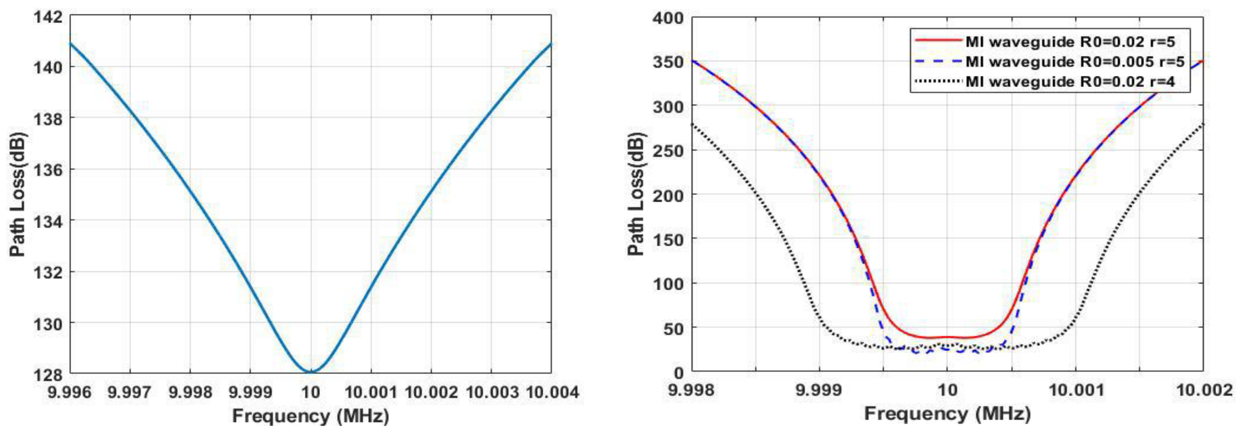

(a) (b)

Figure 10. (a) Frequency response of the MI system. (b) Frequency response of the MI waveguide system with different wire resistance and relay distance.

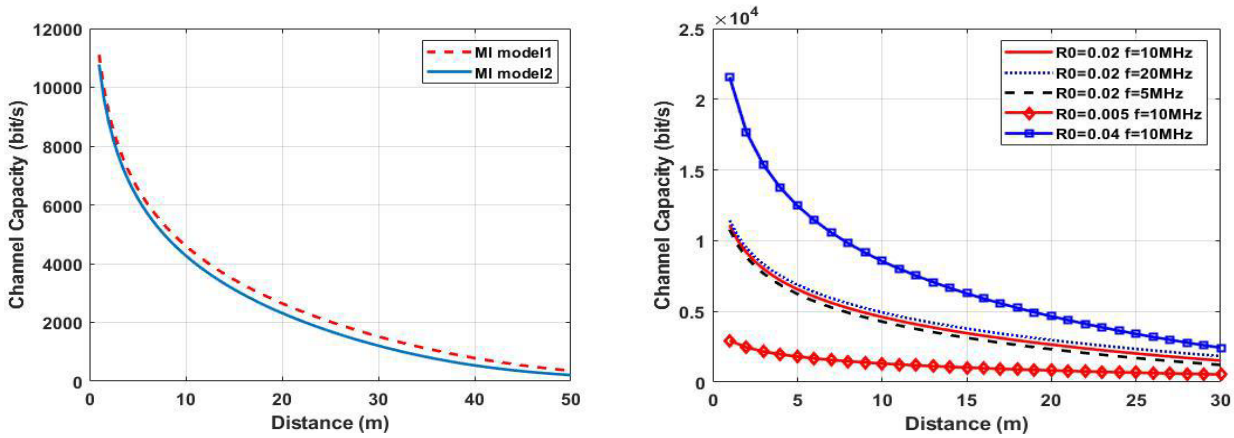

(a) (b)

Figure 11. (a) Channel Capacity of the two models of magnetic induction systems. (b) Channel Capacity of the MI system with different wire resistances and frequencies.

In the magnetic induction waveguide system, the path loss at frequency $f_0 + 0.5B$ is twice as much as the path loss at the center frequency f_0, which can be obtained by formula (5):

$$\left| \frac{\zeta\left(\dfrac{R + j2\pi(f_0+0.5B)L + \dfrac{1}{j2\pi(f_0+0.5B)L}}{2\pi f M}, n-1\right)}{\zeta\left(\dfrac{R}{2\pi f_0 M}, n-1\right)} \right| = \sqrt{2} \tag{18}$$

When the relay coil distance is large, the influence of the highest order variable in the polynomial is the largest, and the bandwidth B is much smaller than the center frequency f_0. Therefore, Eq. (18)

is approximate:

$$\left| \frac{R + j2\pi(f_0 + 0.5B)L + \dfrac{1}{j2\pi(f_0 + 0.5B)L}}{R} \right|^{(n-1)} = \sqrt{2} \tag{19}$$

Then the bandwidth and capacity of the magnetic induction waveguide system are expressed as [17]

$$B \simeq \frac{R}{\mu\pi^2 a}\sqrt{2^{(n-1)^{-1}} - 1} \quad C \simeq \frac{R}{\mu\pi^2 a}\sqrt{2^{(n-1)^{-1}} - 1} \cdot \log\left[1 + \frac{P_r}{N_0}\right] \tag{20}$$

where received power P_r is given by Equation (5); the transmission power is set to 10 dBm; the noise power is set to −105 dBm. Fig. 12 shows the channel capacity of the magnetic induction waveguide with different coil resistances R and coil spacings r. It can be found that reducing the coil resistance can reduce the path loss, but it will also reduce the bandwidth; increasing the spacing between coils will increase the bandwidth, but also increase the path loss. Therefore, there is an optimal coil resistance and coil spacing to maximize the channel capacity.

Figure 13 shows that the relationship between channel capacity and transmission distance of the magnetic induction waveguide system under different coil radii and operating frequencies. Different from

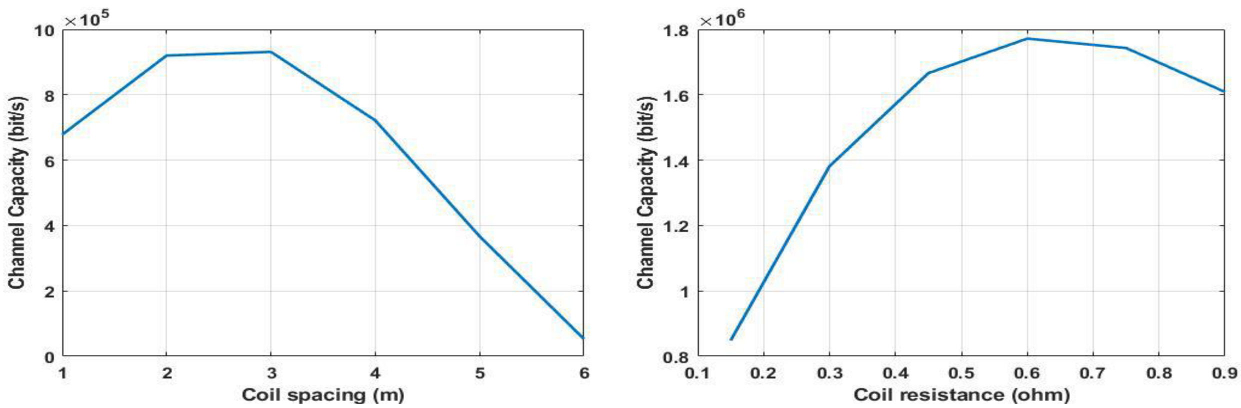

(a) (b)

Figure 12. (a) Channel Capacity as a function of coil spacing. (b) Channel Capacity as a function of coil resistance.

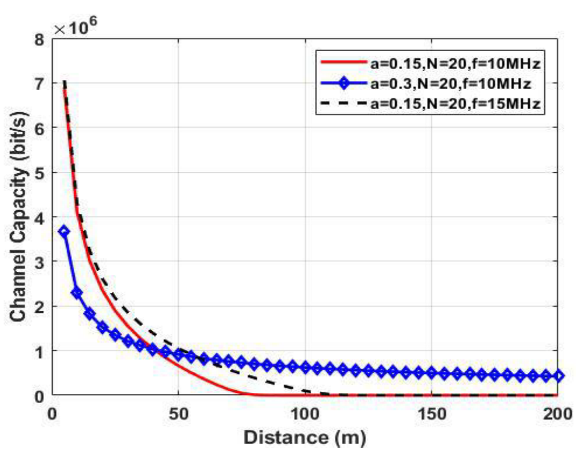

Figure 13. The relationship between channel capacity and transmission distance for different coil radii and operating frequencies.

the traditional wireless channel, the signal-to-noise ratio and bandwidth decrease significantly with the increase of transmission distance, so the channel capacity decreases rapidly. Increasing the coil radius can reduce the bandwidth and greatly reduce path loss, especially in the long-distance transmission. Therefore, increasing the coil radius will reduce the channel capacity, but the attenuation speed is slow. Increasing the working frequency can increase mutual inductance and improve the channel capacity to some extent.

4. CONCLUSION

The Conclusion is based on the numerical comparisons of the EM wave and MI communication system results, illustrated in the figures.

(1) When the transmission distance is the same, the vertical component of the magnetic field generated by the underground loop is larger than that generated by the ground loop. For the earth with low conductivity, the difference between the two is small, but for the earth with high conductivity, the difference is large.

(2) The path losses of the two magnetic induction models are similar. When the conductivity is large, the path loss of the electromagnetic wave is obviously greater than that of magnetic induction communication. Even in a low conductivity environment, when the transmission distance is large enough, the magnetic induction system has a path loss smaller than the electromagnetic wave, and the electromagnetic wave has a higher working efficiency at lower frequencies, while the magnetic induction system is more suitable for working at higher frequencies.

(3) The magnetic induction waveguide technology can greatly reduce the path loss, and the path loss can be further reduced by reducing the distance and resistance of the relay coil. When the transmission distance is relatively short, increasing the number of relay coils will have no obvious effect and cause greater path loss. When the transmission distance is relatively large, increasing the number of relay coils will have a good effect on reducing the path loss.

(4) The bandwidth of the magnetic induction communication system is similar to that of the magnetic induction waveguide system, and both of them are small. The bandwidth of the magnetic induction waveguide system can be increased by reducing the relay distance.

(5) The channel capacities of the two models of magnetic induction system are similar, and the frequency has less influence on the capacity, while the line resistance has more influence on the capacity. The channel capacity can be increased by increasing the line resistance. For the magnetic induction waveguide system, there is an optimal coil resistance and coil spacing to maximize the channel capacity.

REFERENCES

1. Akyildiz, I. F. and E. P. Stuntebeck, "Wireless underground sensor networks: Research challenges," *Ad Hoc Netw.*, Vol. 4, No. 6, 669–686, 2006.
2. Shi, W. J., Y. J. Sun, and S. Li, "Theory and Key technology of wireless magnetic induction sensor network in challenging environment," *Industry and Mine Automation*, Vol. 42, No. 6, 20–25, 2016.
3. Akyildiz, I. F. and E. P. Stuntebeck, "Underground wireless communication using magnetic induction," *IEEE ICC*, 1–5, 2009.
4. Jack, N. and K. Shenai, "Magnetic induction ic for wireless communication in RF-impenetrable media," *IEEE WMED*, Vol. 13, No. 4, 47–48, 2007.
5. Sun, Z. and I. F. Akyildiz, "Optimal deployment for magnetic induction-based wireless networks in challenged environments," *IEEE Trans. Wirel. Commun.*, Vol. 12, No. 3, 996–1005, 2013.
6. Akyildiz, I. F., W. Su, and Y. Sankarasubramaniam, "Wireless sensor networks: A survey," *Comput. Netw.*, Vol. 38, 393–422, 2002.
7. Kalinin, V. A., K. H. Ringhofer, and L. Solymar, "Magneto-inductive waves in one, two, three dimensions," *J. Appl. Phys.*, Vol. 92, No. 10, 6525–6261, 2002.
8. Sun, Z. and I. F. Akyildiz, "Underground wireless communication using magnetic induction," *IEEE ICC*, 1–5, Dresden, Germany, June 2009.

9. Sun, Z. and I. F. Akyildiz, "Magnetic induction communications for wireless underground sensor networks," *IEEE Trans. Antenn. Propag.*, Vol. 58, No. 7, 2426–2435, 2010.
10. Agbinya, J. I. and M. Masihpour, "Magnetic induction channel models and link budgets: A comparison between two Agbinya-Masihpour models," *Third International Conference on Communications and Electronics (ICCE)*, 400–405, 2010.
11. Masihpour, M. and J. I. Agbinya, "Cooperative relay in near field magnetic induction: A new technology for embedded medical communication systems," *The Fifth International Conferenceon Broadband and Biomedical Communications*, 1–6, 2010.
12. Johnson, I. A. and M. Masihpour, "Power equations and capacity performance of magnetic induction communication systems," *IB2Com'10 Conference*, 1–6, Malaga, Spain, 2010.
13. Agbinya, J. I., "A magneto-inductive link budget for wireless power transfer and inductive communication systems," *Progress In Electromagnetics Research C*, Vol. 37, 15–28, 2013.
14. Wait, J. R. and K. Spies "Subsurface electromagnetic fields of a circular loop of current located above ground," *IEEE Trans. Antenn. Propag.*, Vol. 20, No. 4, 520–522, 1972.
15. Yan, L. Y., J. A. Waynert, and C. Sunderman, "Measurements and modeling of through-the-earth communications for coal mines," *IEEE Trans. Ind. Appl.*, Vol. 49, No. 5, 1979–1983, 2013.
16. Li, L., M. C. Vuran, and I. F. Akyildiz, "Characteristics of underground channel for wireless underground sensor networks," *Med-Hoc-Net'07*, 92–99, Corfu, Greece, June 2007.
17. Sun, Z. and I. F. Akyildiz, "On capacity of magnetic induction-based wireless underground sensor networks," *2012 Proceedings of the IEEE INFOCOM*, 370–378, Orlando, USA, 2012.